



A novel vapor–liquid segmented flow based on solvent partial vaporization in microstructured reactor for continuous synthesis of nickel nanoparticles

Changfeng Zeng^a, Chongqing Wang^b, Fang Wang^c, Yu Zhang^b, Lixiong Zhang^{b,*}

^a College of Mechanic and Power Engineering, Nanjing University of Technology, No. 5 Xin Mofan Rd., Nanjing 210009, China

^b State Key Laboratory of Materials-Oriented Chemical Engineering, College of Chemistry and Chemical Engineering, Nanjing University of Technology, Nanjing 210009, PR China

^c College of Science, Nanjing University of Technology, Nanjing 210009, PR China

HIGHLIGHTS

- ▶ Ni nanoparticles were synthesized in a microreactor by chemical reduction in 4 min.
- ▶ A vapor–liquid segmented flow was formed based on partial vaporization of solvent.
- ▶ The size of nickel nanoparticles is ca. 80 nm with narrow particle size distribution.

ARTICLE INFO

Article history:

Received 23 May 2012

Received in revised form 11 July 2012

Accepted 20 July 2012

Available online 28 July 2012

Keywords:

Nickel nanoparticle

Segmented flow

Microreactor

Partial vaporization

Chemical reduction

ABSTRACT

Continuous synthesis of nickel nanoparticles was conducted in a microstructured reactor by chemical reduction of nickel chloride dissolved in ethanol by hydrazine hydrate. A novel vapor–liquid segmented flow method was thus developed based on partial vaporization of the ethanol in the reaction system, leading to formation of nickel nanoparticles in a smooth manner without clogging. The effect of the residence time, the reaction temperature and addition of surfactant was examined. Nickel nanoparticles with mean diameters of about 80 nm and narrow particle size distributions could be synthesized at 60–75 °C within 4 min. Addition of cetyltrimethylammonium bromide in the reaction system resulted in further decrease in the particle size to 68 nm. The nickel nanoparticles exhibit superior catalytic activities to the commercial used Raney Ni catalyst in hydrogenation of *p*-nitrophenol to *p*-aminophenol.

© 2012 Elsevier B.V. All rights reserved.

1. Introduction

Nano-metal materials, with unique chemical and physical properties compared to those of their corresponding bulk materials, are widely used in catalytic, electronic and magnetic fields [1–4]. Morphology and size control of nano-metal materials is a very significant objective because their unique properties are largely dependent on their sizes and shapes. In view of the importance of these materials, diverse preparation methods have been developed for the synthesis of metal nanoparticles, including chemical reduction [5], photochemical reduction [6], reverse micelle method [7], template directed method [8], and electrochemical technique [9]. Among them, the solution-phase chemical reduction method is quite efficient and widely used owing to its low cost, high yield, and simplicity. Batch reactors are conventionally used for the solution-phase chemical reduction, which suffers from difficulties in avoiding secondary nucleation and aggregation, thus resulting in

a broad particle size distribution, because of inhomogeneous temperature distributions and insufficient mixing.

In recent years, microstructured reactors have attracted increasing interest resulting from their high heat and mass transfer rates over batch reactors, and easy control of experimental conditions such as pressure, temperature, residence time, and flow rate. A couple of fabrication techniques are thus developed for the manufacture of these microreactors [10–15]. They are quite commonly applied in systems as organic synthesis, in which the raw materials and products are in the state of liquid or gas. On the other hand, microstructured reactors are more and more used in the production of micro- and nano-sized particles [16–20], including metal nanoparticles [21–31]. As a homogeneous reaction environment can be realized in the microreactors, monodisperse metal nanoparticles can be easily produced, as demonstrated in the recent publications for continuous flow synthesis of nano-sized gold [21–24], silver [25–27], cobalt [28,29], palladium [30], and copper [31] in microfluidic devices. Moreover, microstructured reactors exhibit an advantage in transition from lab-scale to industrial-scale processes by a numbering-up rather than scale-up solution. However, clogging of

* Corresponding author. Tel.: +86 25 8317 2265; fax: +86 25 8317 2263.

E-mail address: lixiongzhang@yahoo.com (L. Zhang).

the microchannels in the microstructured reactors is an important issue which has to be taken into consideration for preparation of nanoparticles in these reactors. One of the solutions to this issue is to create a two-phase segmented flow pattern in microchannels so that the solid products synthesized in an aqueous phase can be kept away from inner wall of the tube by a gas or oil phase [32–39]. Furthermore, mixing in the segmented microdroplets is intensified and axial dispersion is eliminated, leading to formation of the products with more uniform particle size distribution. Liquid–liquid segmented flow systems are operated using insoluble liquids as a separated medium. However, separation of the insoluble liquids makes the synthesis processes more complex. Thus, gas–liquid segmented flow systems are more attractive because of easy separation of the gas from the liquid, but recycle of the gas needs additional equipment such as a compressor and a desiccator.

In this paper, we presented a novel method to create a vapor–liquid segmented flow system in a microstructured reactor by partially vaporizing the solvent in the reactants at suitable temperatures for preparation of nickel nanoparticles in an alcohol solution. No oil or inert gas is introduced in the reaction system, eliminating recycle of the oil or gas. The synthesis of nickel nanoparticles by reducing nickel salts with hydrazine hydrate by this method in the microstructured reactor was taken as an example to demonstrate the feasibility of this method since the price of the nickel precursor is relatively cheap. Furthermore, nickel nanoparticles is of particular interest because of their wide applications in conducting paints [40], rechargeable batteries [41], hydrogenation catalyst [42], and so on. So far, the synthesis of nickel nanoparticles in microstructured reactors has been rarely reported [43]. We conducted synthesis of nickel nanoparticles using ethanol as the solvent at this operation mode for a couple of hours. The effects of some operation parameters on the particle size and particle size distribution were also explored. The catalytic activities of the resultant products in hydrogenation of *p*-nitrophenol to *p*-aminophenol were examined and compared with the commercial used Raney Ni catalyst. Nickel nanoparticles with narrow particle size distributions were successfully prepared without clogging.

2. Experimental section

2.1. Synthesis of nickel nanoparticles

Nickel nanoparticles were synthesized in a microstructured reactor by the reduction of nickel chloride dissolved in ethanol using hydrazine hydrate (N_2H_4) as a reducing agent. A schematic of the microreaction process, a caterpillar mixer (IMM, Germany), and the flow patterns in the microstructured reactor are shown in Fig. 1. First, a 0.4 mol L^{-1} NiCl_2 solution was prepared by dissolving $\text{NiCl}_2 \cdot 6\text{H}_2\text{O}$ in ethanol. A hydrazine hydrate solution was prepared by dissolving NaOH in a hydrazine hydrate and ethanol mixture, with both the NaOH and hydrazine hydrate concentrations being 1.6 mol L^{-1} . When a surfactant such as cetyltrimethylammonium bromide (CTAB) and poly(vinylpyrrolidone) (PVP) was used, it was dissolved in the NiCl_2 solution. The two solutions were introduced into the caterpillar mixer connected with a fluorinated-ethylene-propylene (FEP) tube with an inner diameter of 1 mm as a residence time delay loop at its outlet using two high performance liquid chromatography (HPLC) pumps at a total flow rate of 8 mL min^{-1} with a flow rate ratio of 1:1. Both the mixer and the delay loop were immersed in an oil bath controlled at a designed temperature. The produced particles were centrifuged and washed with distilled water and ethanol, and finally dried in an oven at 80°C . Care should be taken for handling the dried product since the nickel nanoparticles are carcinogenic.

2.2. Characterization of nickel nanoparticles

Transmission electron microscopy (TEM) observation of the nickel nanoparticles was conducted on a JEM22000 electron microscope. The sample was prepared by dropping the re-dispersed nickel nanoparticle alcohol solution onto a copper grid coated with carbon film. The nanoparticle crystal structures were characterized by selected area electron diffraction (SAED) and X-ray diffraction (XRD) on Bruker D8-advanced diffractometer equipped with a $\text{Cu K}\alpha$ X-ray source operating at 40 kV and 30 mA. Flow patterns of the vapor–liquid segments in the FEP tube were recorded by macro lenses (Pentax, Japan) connected to a high-speed CCD video camera with a frequency of 50 images per second. The particle size distribution was analyzed by measuring between 250 and 400 nanoparticles based on TEM micrographs using Scion Image Software 4.0.2 (Scion Corp).

The catalytic properties of the nickel nanoparticles for hydrogenation of *p*-nitrophenol to *p*-aminophenol were evaluated in a 100 ml stainless-steel autoclave with an electromagnetic stirrer and a temperature control unit (Parr). Comparison with commercially used Raney Ni (Anhui Ba Yi Chemical Company, China) was also conducted under the same condition. First, 0.02 g of the nickel nanoparticles and 1.0 g of *p*-nitrophenol were charged in 40 ml ethanol pre-filled in the autoclave. Then, the autoclave was sealed and purged with hydrogen three times to remove air. Afterwards, the reactor was heated to 100°C at low stirring speed (100 rpm). When the temperature reached the set point, hydrogen gas was introduced into the reactor to 1.6 MPa, and the stirring speed was increased to 800 rpm. After no uptake of H_2 was observed (by monitoring the system pressure), the reactor was cooled to room temperature and samples were taken from the reaction system. The solid particles were immediately separated from the solution by centrifugation. The liquid products were analyzed using a HPLC system equipped with an ultraviolet detector set at a wavelength of 270 nm and an auto-sampler (Agilent 1100 series). Chromatographic separations were performed at 35°C using a ZARBOX Eclipse XDB-C18, $5 \mu\text{m}$, $4.6 \text{ mm} \times 250 \text{ mm}$ column. A mobile phase composed of 65% methanol and 35% water at a flow rate of 1 mL min^{-1} was used. The catalytic activity of the nickel nanoparticles was calculated by dividing the converted mol of *p*-nitrophenol by the mol of the Ni amount and the reaction time.

3. Results and discussions

Generally, preparation of nickel nanoparticles by chemical reduction is conducted by addition of reduction agents, such as hydrazine hydrate or sodium boron hydride into aqueous solution of nickel salt at $70\text{--}90^\circ\text{C}$. We first tried to carry out this reaction by introducing a NiCl_2 aqueous solution and a hydrazine hydrate aqueous solution into two inlets of the microstructured reactor at 70°C . We observed formation of discontinuous liquid flow, segmented by gas bubbles produced from hydrazine hydrate. Nevertheless, the reactor was quickly clogged. This problem could not be solved even after intensive examination of experimental parameters. We believed this results from discontinuous segmented flow. We thus conducted the above experiments by using ethanol instead water as the solvent. The concentrations of $\text{NiCl}_2 \cdot 6\text{H}_2\text{O}$ and NaOH ethanol solutions were 0.4 and 1.6 mol L^{-1} , respectively, with a $\text{Ni}^{2+}:\text{N}_2\text{H}_4$ molar ratio of 1:4 and N_2H_4 dissolved in the NaOH solution. The reaction temperature was set at 70°C . We observed formation of uniform segments among the black liquid flow (Fig. 1c). The experiment could be continuously carried out for a couple of hours without occurrence of clogging of the reactor, suggesting that partial vaporization of the ethanol solvent plays an important role in continuous flow synthesis.

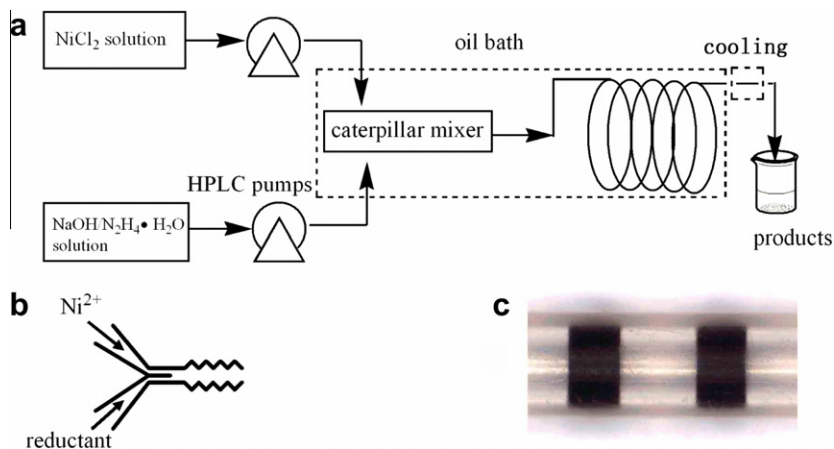


Fig. 1. The schematic of the microreaction process (a), the caterpillar mixer (b), and the flow pattern in the microstructured reactor (c).

Fig. 2a shows the XRD patterns of the samples produced under the above experimental conditions at the residence times of 0.78–3.9 min and the reaction temperature of 70 °C. All the samples exhibit diffraction peaks at $2\theta = 44.5^\circ$, 51.8° , and 76.3° corresponding to the Ni (111), Ni (200), and Ni (220) faces, respectively, indicating formation of Ni. However, the samples prepared at the residence times of 0.78 and 1.2 min show diffraction peaks of $\text{Ni}(\text{OH})_2$ appeared at $2\theta = 33.1^\circ$, 38.4° and 59.0° , corresponding to the (100), (101) and (111) faces, suggesting insufficient time for reduction of nickel salts. No characteristic diffraction peaks of $\text{Ni}(\text{OH})_2$ were observed from these samples produced at residence times of 2.4 and 3.9 min. Fig. 2b and c shows the TEM image and particle size distribution of the sample prepared at the residence time of 3.9 min. We could observe that the particles are in nanometer range, with a mean diameter of 80 nm and a particle size distribution ranging from 60 to 114 nm. No nickel ion was detected in the residual solution, suggesting complete reduction of the nickel salt. Thus, about 11.5 g/h of nickel nanoparticles can be produced in this simple setup. These

results demonstrate that the nanometer sized nickel particles could be successfully prepared in the microstructured reactor based on vapor–liquid segmented flow microreaction using hydrazine hydrate as a reducing agent.

In order to explore the effect of reaction temperature on the synthesis of nickel nanoparticles, experiments were carried out at 60 and 75 °C and a residence time of 3.9 min in the same microstructured reactor with the same concentration and flow rates of the reactants. Under such experimental conditions, we observed that the flow was stable for about 5 min. Then a sudden pulse occurred for about 1 s and the flow was stable again. This can be ascribed to the condensation of the vapor bubbles during the cooling [44]. Continuous preparation of nano-sized nickel particles could also be implemented at the reaction temperature of 60 °C with vapor–liquid segmented flow pattern in the microreactor, although the boiling point of ethanol is 78.4 °C, indicating partial vaporation of ethanol at this temperature. XRD characterization of the products shows formation of pure nickel. Their TEM images shown in Fig. 3a and b indicate that the nickel particles have good disper-

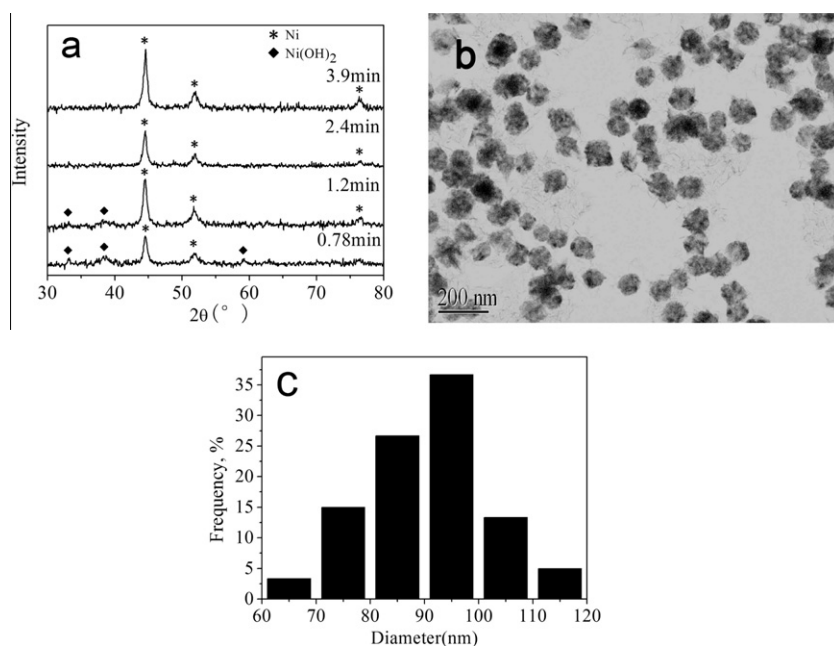


Fig. 2. XRD patterns of the samples produced in the microreactor at 70 °C and different residence times (a) and TEM image (b) and particles size distribution of nickel nanoparticles (c) prepared in the microreactor at 70 °C and a residence time of 3.9 min.

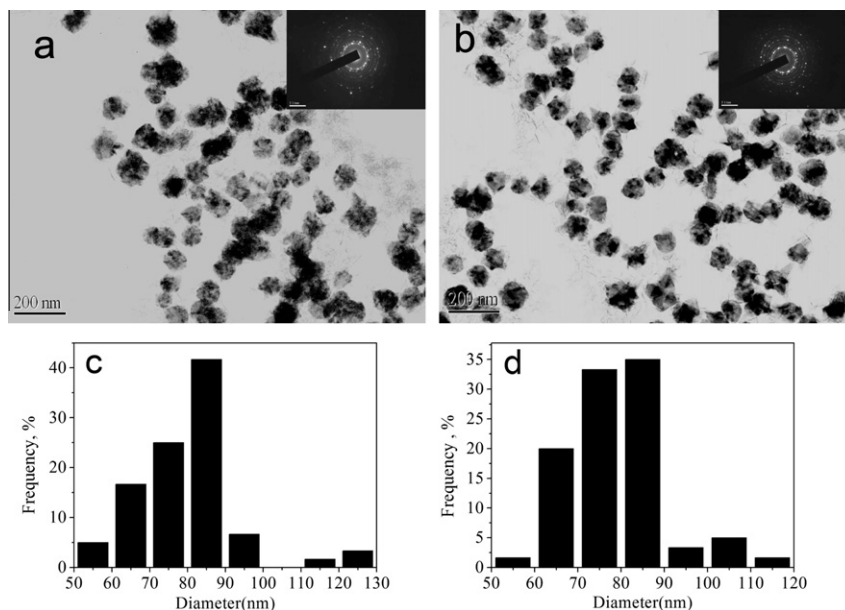


Fig. 3. TEM images (a and b) and the corresponding SAED patterns (insets in a and b) and particle size distributions (c and d) of the nickel nanoparticles synthesized at the reaction temperatures of 60 °C (a and c) and 75 °C (b and d).

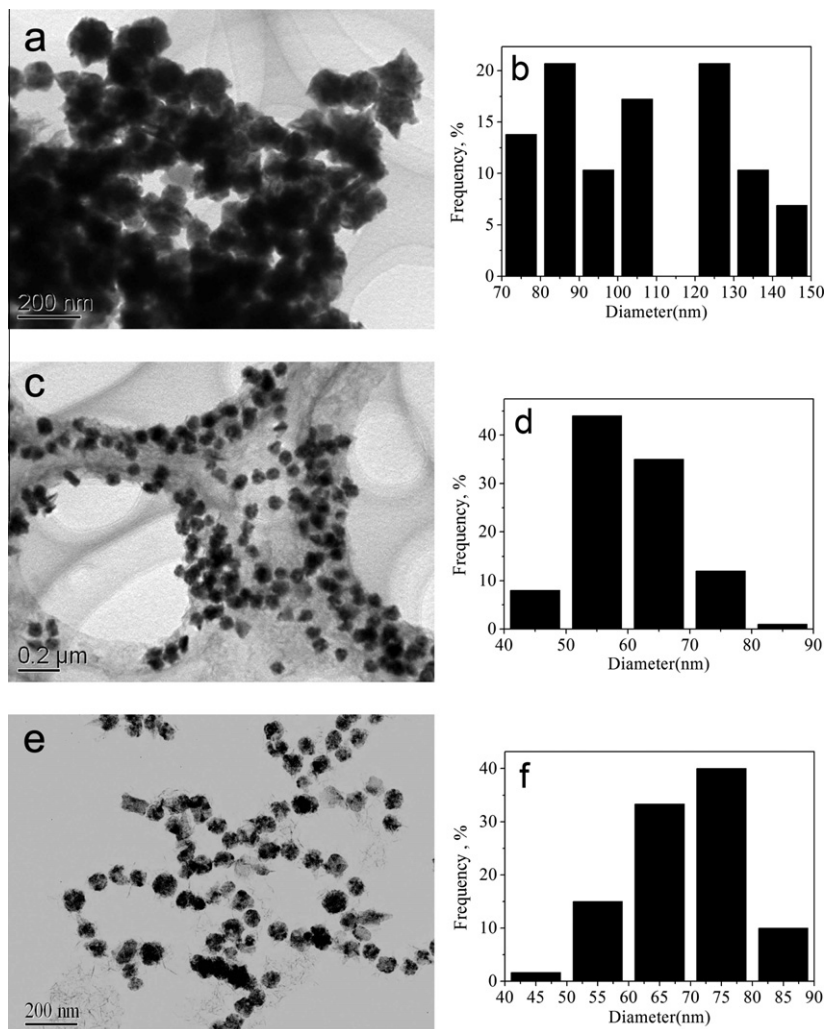


Fig. 4. TEM images (a, c, e) and particle size distributions (b, d, f) of nickel nanoparticles prepared using PVP with a PVP/Ni²⁺ molar ratio of 0.5 (a, b) and CTAB with a CTAB/Ni²⁺ molar ratio of 0.25 (c, d) and a CTAB/Ni²⁺ molar ratio of 0.5 (e, f).

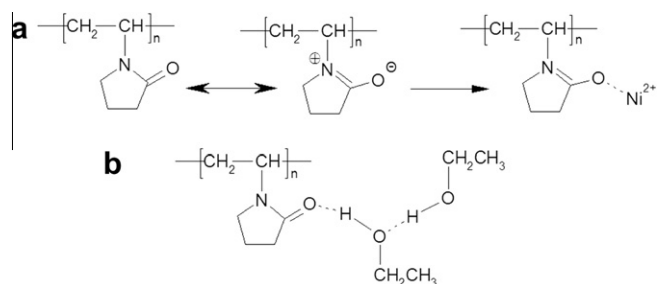


Fig. 5. A proposed mechanism of interaction between PVP and nickel ions (a) and interaction between PVP and ethanol (b).

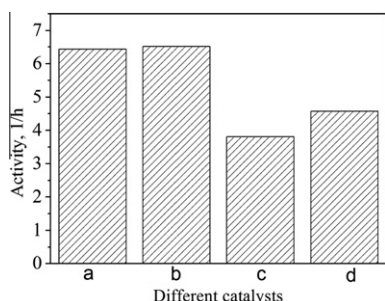


Fig. 6. The catalytic activities of nickel nanoparticles prepared at 70 °C without addition of surfactant (a), with addition of CTAB (b) and PVP (c) and their comparison with that of the commercial used Raney Ni (d).

sion. The corresponding SAED patterns shown also in Fig. 3a and b (insets) demonstrate bright diffraction rings, revealing that the nickel nanoparticles prepared at the two temperatures are polycrystalline with a high degree of crystallinity. Their particle size distributions (Fig. 3c and d) indicate that the mean diameters of nickel nanoparticles produced at the reaction temperature of 60 and 75 °C are 84 and 78 nm, with the particle size distribution ranging from 56 to 129 nm and from 58 to 111 nm, respectively. By comparing these results with those obtained at the reaction temperature of 70 °C, we could conclude that the mean diameter of the nickel nanoparticles slightly decreases with increase in the reaction temperature. This could be explained by the fact that the nucleation rate is higher at higher reaction temperature, thus producing larger amount of nuclei while inhibiting the nuclei growth, and in turn favoring formation of smaller nanoparticles. Similar trend was also observed in the synthesis of silver in a continuous flow tubular microreactor using silver pentafluoropropionate as a single-phase reactant precursor [45]. The particle size distribution of the nickel nanoparticles also slightly decreases with increase in reaction temperature. This trend is different from the synthesis of silver in the microreactor, where the size distributions of the particles formed at the high temperature were relatively broadened [45]. This may result from the segmented flow in our microreactor, which favors formation of particles with narrow particle size distribution [32–39].

To further adjust the particle size and particle size distribution of the nickel nanoparticles, CTAB and PVP, which were previous revealed to have strong influence on the particle size and particle size distribution in the synthesis of nanoparticles [46], were added in the reaction system with the reaction conducted at the reaction temperature of 70 °C and residence time of 3.9 min and CTAB/ Ni^{2+} and PVP/ Ni^{2+} molar ratios of 0.5. Fig. 4 shows TEM images and the corresponding particle size distributions of the prepared nickel nanoparticles. It was obvious from the TEM images that all the products exhibit spherical morphology with different particle

sizes. When PVP was used, a significant aggregation of nanoparticles could be observed, leading to large particles with the mean particle size of 104 nm, and a broad particle size distribution ranging from 70 to 140 nm. This is different from the trend in conventional batch synthesis of nickel synthesis using the same method but with water as the solvent [47]. In an aqueous system, PVP, as the dispersant agent, interacts with the nickel ions by the strong ionic bonds between the metallic ions and the amide group in PVP [48], as shown in Fig. 5a. In this investigation, however, ethanol was used as the solvent, which forms hydrogen bonds with the carbonyl groups of PVP through the hydroxyl groups of ethanol [49], as shown in Fig. 5b. Under such circumstance, the nickel ions and the formed nickel nanoparticles are not dispersed, resulting in aggregation. On the other hand, usage of CTAB results in obvious decrease in both the mean diameter and particle size distribution of the corresponding product. Nickel nanoparticles with a mean diameter of 60 nm and particle size distribution ranging from 40 to 80 nm were produced. We further decreased the CTAB/ Ni^{2+} molar ratio to 0.25. The resulting nickel nanoparticles show a slight increase in the mean particle size to 68 nm without obvious change in the particle size distribution, suggesting higher CTAB concentration favors formation of smaller sized nickel nanoparticles. The above results suggest that surfactants have notable effect on the particle size and particle size distribution of the nickel nanoparticles without apparent influence on their morphology, exhibiting that CTAB could inhibit the growth of particles while PVP could enhance aggregation of the particles.

Fig. 6 shows the catalytic activities of different nickel nanoparticles prepared at 70 °C and a residence time of 3.9 min with and without addition of surfactants and commercially used Raney Ni catalyst. Obviously, the nickel particles obtained without addition of surfactant and with addition of CTAB have quite similar activities, with the latter being slightly higher than the former. The nickel particles obtained with addition of PVP exhibit much lower activity than those obtained without addition of surfactant and with addition of CTAB, quite possibly corresponding to their aggregated particles and large particle sizes. These results are correlated well with the particle sizes of the nickel nanoparticles. In addition, the nickel nanoparticles obtained without addition of surfactant and with addition of CTAB exhibit higher than the commercially used Raney Ni catalyst, demonstrating potential application of these nanoparticles as catalysts.

4. Conclusions

We developed a novel vapor–liquid segmented flow method for synthesis of nanoparticles in microstructured reactors to avoid clogging of the microchannels. Nickel nanoparticles could be continuously synthesized by this method. The mean diameter and the particle size distribution of the nanoparticles could be adjusted by tuning experimental parameters such as reaction temperature and addition of suitable surfactant. Increasing reaction temperature resulted in smaller particles size and narrower particle size distribution. Addition of CTAB as a surfactant led to decrease in the particle size and particle size distribution. We believe that this method can be used in the synthesis of other kinds of nanoparticles in microstructured reactors.

Acknowledgments

This work is supported by SRFPD (20093221110002), Natural Science Key Project of the Jiangsu Higher Education Institutions (12KJA530002) and the Priority Academic Program Development of Jiangsu Higher Education Institutions.

References

- [1] C.J. Wang, M. Shim, P. Guyot-Sionnest, Electrochromic nanocrystal quantum dots, *Science* 291 (2001) 2390–2392.
- [2] M. Shim, P. Guyot-Sionnest, N-type colloidal semiconductor nanocrystals, *Nature* 407 (2000) 981–983.
- [3] A.L. Wang, H.B. Yin, H.H. Lu, J.J. Xue, M. Ren, T.S. Jiang, Effect of organic modifiers on the structure of nickel nanoparticles and catalytic activity in the hydrogenation of *p*-nitrophenol to *p*-aminophenol, *Langmuir* 25 (2009) 12736–12741.
- [4] V.I. Klimov, A.A. Mikhailovsky, S. Xu, A. Malko, J.A. Hollingsworth, C.A. Leatherdale, H.J. Eisler, M.G. Bawendi, Optical gain and stimulated emission in nanocrystal quantum dots, *Science* 290 (2000) 314–317.
- [5] T. Yonezawa, S. Onoue, N. Kimizuka, Preparation of highly positively charged silver nanoballs and their stability, *Langmuir* 16 (2000) 5218–5220.
- [6] H.H. Huang, X.P. Ni, G.L. Loy, C.H. Chew, K.L. Tan, F.C. Loh, J.F. Deng, G.Q. Xu, Photochemical formation of silver nanoparticles in poly(*n*-vinylpyrrolidone), *Langmuir* 12 (1996) 909–912.
- [7] W. Wang, S. Efrima, O. Regev, Directing oleate stabilized nanosized silver colloids into organic phases, *Langmuir* 14 (1998) 602–610.
- [8] N.R. Jana, L. Gearheart, C.J. Murphy, Evidence for seed-mediated nucleation in the chemical reduction of gold salts to gold nanoparticles, *Chem. Mater.* 13 (2001) 2313–2322.
- [9] M.T. Reetz, W. Helbig, Size-selective synthesis of nanostructured transition metal clusters, *J. Am. Chem. Soc.* 116 (1994) 7401–7402.
- [10] K.D. Wise, K. Najafi, Microfabrication techniques for integrated sensors and microsystems, *Science* 254 (1991) 1335.
- [11] M. Madou, *Fundamentals of Microfabrication*, CRC Press, New York, 1997. pp. 145–215.
- [12] R.D. Piner, J. Zhu, F. Xu, S. Hong, C.A. Mirkin, Dip-Pen nanolithography, *Science* 283 (1999) 661.
- [13] J.L.H. Chau, Y.S.S. Wan, A. Gavriilidis, K.L. Yeung, Incorporating zeolites in microchemical systems, *Chem. Eng. J.* 88 (2002) 187–200.
- [14] Y.S.S. Wan, J.L.H. Chau, A. Gavriilidis, K.L. Yeung, Design and fabrication of zeolite-based microreactors and membrane microseparators, *Microporous Mesoporous Mater.* 42 (2001) 157–175.
- [15] W. Han, S.M. Kwan, K.L. Yeung, Zeolite applications in fuel cells: water management and proton conductivity, *Chem. Eng. J.* 187 (2012) 367–371.
- [16] S. Li, S. Meierott, J.M. Köhler, Effect of water content on growth and optical properties of ZnO nanoparticles generated in binary solvent mixtures by micro-continuous flow synthesis, *Chem. Eng. J.* 165 (2010) 958–965.
- [17] J. Ju, C. Zeng, L. Zhang, N. Xu, Continuous synthesis of zeolite NaA in a microchannel reactor, *Chem. Eng. J.* 116 (2006) 115–121.
- [18] C.K. Chung, T.R. Shih, C.K. Chang, C.W. Lai, B.H. Wu, Design and experiments of a short-mixing-length baffled microreactor and its application to microfluidic synthesis of nanoparticles, *Chem. Eng. J.* 168 (2011) 790–798.
- [19] P.M. Günther, G.A. Groß, J. Wagner, F. Jahn, J.M. Köhler, Introduction of surface-modified Au-nanoparticles into the microflow-through polymerization of styrene, *Chem. Eng. J.* 135 (2008) S126–S130.
- [20] S.-T. Tu, X. Yu, W. Luan, H. Löwe, Development of micro chemical, biological and thermal systems in China: a review, *Chem. Eng. J.* 163 (2010) 165–179.
- [21] J. Wagner, T. Kirner, G. Mayer, J. Albert, J.M. Köhler, Generation of metal nanoparticles in a microchannel reactor, *Chem. Eng. J.* 101 (2004) 251–260.
- [22] D. Shalom, R.C.R. Wootton, R.F. Winkle, B.F. Cottam, R. Vilar, A.J. deMello, C.P. Wilde, Synthesis of thiol functionalized gold nanoparticles using a continuous flow microfluidic reactor, *Mater. Lett.* 61 (2007) 1146–1150.
- [23] J. Wagner, J.M. Köhler, Continuous synthesis of gold nanoparticles in a microreactor, *Nano Lett.* 5 (2005) 685–691.
- [24] S. Duraiswamy, S.A. Khan, Droplet-based microfluidic synthesis of anisotropic metal nanocrystals, *Small* 5 (2009) 2828–2834.
- [25] J. Wagner, T.R. Tshikhudo, J.M. Köhler, Microfluidic generation of metal nanoparticles by borohydride reduction, *Chem. Eng. J.* 135 (2008) S104–S109.
- [26] J.M. Köhler, L. Abahmane, J. Wagner, J. Albert, G. Mayer, Preparation of metal nanoparticles with varied composition for catalytic applications in microreactors, *Chem. Eng. Sci.* 63 (2008) 5048–5055.
- [27] J. Boleininger, A. Kurz, V. Reuss, C. Sonnichsen, Microfluidic continuous flow synthesis of rod-shaped gold and silver nanocrystals, *Phys. Chem. Chem. Phys.* 8 (2006) 3824–3827.
- [28] Y.J. Song, H. Modrow, L.L. Henry, C.K. Saw, E.E. Doomes, V. Palshin, J. Hormes, C. Kumar, Microfluidic synthesis of cobalt nanoparticles, *Chem. Mater.* 18 (2006) 2817–2827.
- [29] Y.J. Song, L.L. Henry, W.T. Yang, Stable amorphous cobalt nanoparticles formed by an in situ rapidly cooling microfluidic process, *Langmuir* 25 (2009) 10209–10217.
- [30] K. Torigoe, Y. Watanabe, T. Endo, K. Sakai, H. Sakai, M. Abe, Microflow reactor synthesis of palladium nanoparticles stabilized with poly(benzyl ether) dendron ligands, *J. Nanopart. Res.* 12 (2010) 951–960.
- [31] Y.J. Song, E.E. Doomes, J. Prindle, R. Tittsworth, J. Hormes, C. Kumar, Investigations into sulfobetaine-stabilized Cu nanoparticle formation: toward development of a microfluidic synthesis, *J. Phys. Chem. B* 109 (2005) 9330–9338.
- [32] S.A. Khan, A. Günther, M.A. Schmidt, K.F. Jensen, Microfluidic synthesis of colloidal silica, *Langmuir* 20 (2004) 8604–8611.
- [33] B.K.H. Yen, A. Gunther, M.A. Schmidt, K.F. Jensen, M.G. Bawendi, A microfabricated gas-liquid segmented flow reactor for high-temperature synthesis: the case of cdse quantum dots, *Angew. Chem. Int. Ed.* 44 (2005). pp. 5447–5451.
- [34] I. Shestopalov, J.D. Tice, R.F. Ismagilov, Multi-step synthesis of nanoparticles performed on millisecond time scale in a microfluidic droplet-based system, *Lab Chip* 4 (2004) 316–321.
- [35] E.M. Chan, A.P. Alivisatos, R.A. Mathies, High-temperature microfluidic synthesis of cdse nanocrystals in nanoliter droplets, *J. Am. Chem. Soc.* 127 (2005) 13854–13861.
- [36] J.R. Burns, C. Ramshaw, The intensification of rapid reactions in multiphase systems using slug flow in capillaries, *Lab Chip* 1 (2001) 10–15.
- [37] Y.C. Pan, M.H. Ju, J.F. Yao, L.X. Zhang, N.P. Xu, Preparation of uniform nano-sized zeolite crystals in microstructured reactors using manipulated organic template-free synthesis solutions, *Chem. Commun.* 46 (2009) 7233–7235.
- [38] Y.C. Pan, J.F. Yao, L.X. Zhang, N.P. Xu, Preparation of ultrafine zeolite crystals with narrow particle size distribution using a two-phase liquid segmented microfluidic reactor, *Ind. Eng. Chem. Res.* 48 (2009) 8471–8477.
- [39] V.S. Cabeza, S. Kuhn, A.A. Kulkarni, K.F. Jensen, Size-controlled flow synthesis of gold nanoparticles using a segmented flow microfluidic platform, *Langmuir* 28 (2012) 7007–7013.
- [40] W.J. Tseng, S.Y. Lin, Effect of polymeric surfactant on flow behaviors of nickel-ethanol-isopropanol suspensions, *Mater. Sci. Eng., A* 362 (2003) 160–166.
- [41] S.H. Park, C.H. Kim, Y.C. Kang, Y.H. Kim, Control of size and morphology in Ni particles prepared by spray pyrolysis, *J. Mater. Sci. Lett.* 22 (2003) 1537–1541.
- [42] A.L. Wang, H.B. Yin, H.H. Lu, J.J. Xue, M. Ren, T.S. Jiang, Catalytic activity of nickel nanoparticles in hydrogenation of *p*-nitrophenol to *p*-aminophenol, *Catal. Commun.* 10 (2009) 2060–2064.
- [43] K. Sue, A. Suzuki, Y. HaKuta, H. Hayashi, K. Arai, Y. Takebayashi, S. Yoda, T. Furuya, Hydrothermal-reduction synthesis of Ni nanoparticles by superrapid heating using a micromixer, *Chem. Lett.* 38 (2009) 1018–1019.
- [44] M. Seo, N. Matsuura, Monodisperse, submicrometer droplets via condensation of microfluidic-generated gas bubbles, *Small* (2012), <http://dx.doi.org/10.1002/smll.201200445>.
- [45] X.Z. Lin, A.D. Terepka, H. Yang, Synthesis of silver nanoparticles in a continuous flow tubular microreactor, *Nano Lett.* 4 (2004) 2227–2232.
- [46] K.H. Kim, Y.B. Lee, S.G. Lee, H.C. Park, S.S. Park, Preparation of fine nickel powders in aqueous solution under wet chemical process, *Mater. Sci. Eng., A* 381 (2004) 337–342.
- [47] J. Gao, F. Guan, Y. Zhao, W. Yang, Y. Ma, X. Lu, J. Hou, J. Kang, Preparation of ultrafine nickel powder and its catalytic dehydrogenation activity, *Mater. Chem. Phys.* 71 (2001) 215–219.
- [48] M.G. Naseri, E.B. Saion, H.A. Ahangar, M. Hashim, A.H. Shaari, Simple preparation and characterization of nickel ferrite nanocrystals by a thermal treatment method, *Powder Technol.* 212 (2011) 80–88.
- [49] R.J. Sengwa, N.M. Abhilasha, More, dielectric relaxation and molecular dynamics in poly(vinylpyrrolidone)-ethylalcohol mixtures in pure liquid state and in non-polar solvent, *Polymer* 44 (2003) 2577–2583.